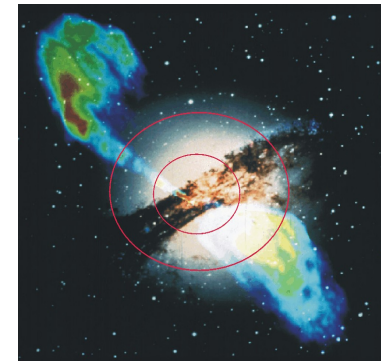


Theoretical Understanding of Blazars

Chuck Dermer (Naval Research Laboratory)

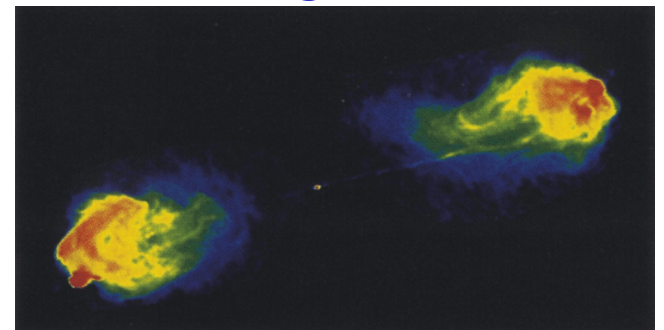
• **Blazars:** class of active galactic nuclei (AGN), including flat spectrum radio quasars, optically violently variable quasars, highly polarized quasars, and BL Lac objects. Blazars are thought to be radio-loud AGN with relativistic jets, powered by supermassive black hole engines, that are aligned towards the observer. EGRET showed that members of the blazar class are luminous gamma-ray sources.

- General Properties
- Evidence for relativistic outflows
- Particle acceleration and radiation processes in blazar jets
- Statistics of blazars
- Relationship to galaxies and AGN
- Black hole/accretion disk/jet physics
- Blazars as sources of ultra-high energy cosmic rays and neutrinos
- Cosmological probes of the diffuse inter-galactic infrared background radiation



Cen A

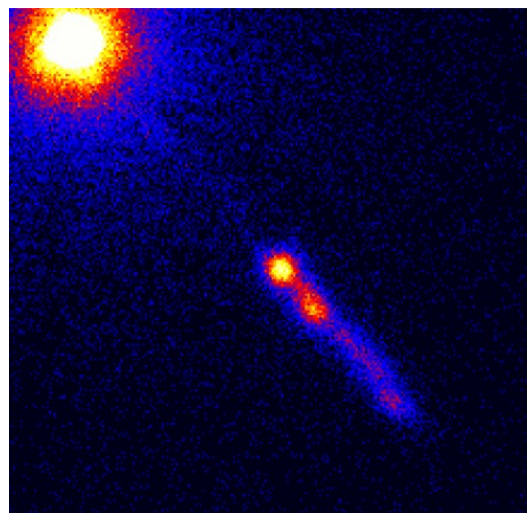
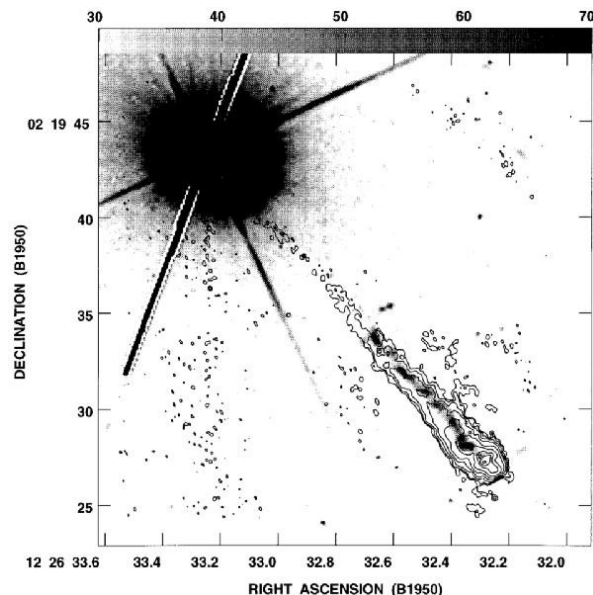
Misaligned blazars



Cyg A

General Properties

Nearby FSRQ: 3C
273



$$z = 0.158,$$

$$d_L = 2.1 \times 10^{27}$$

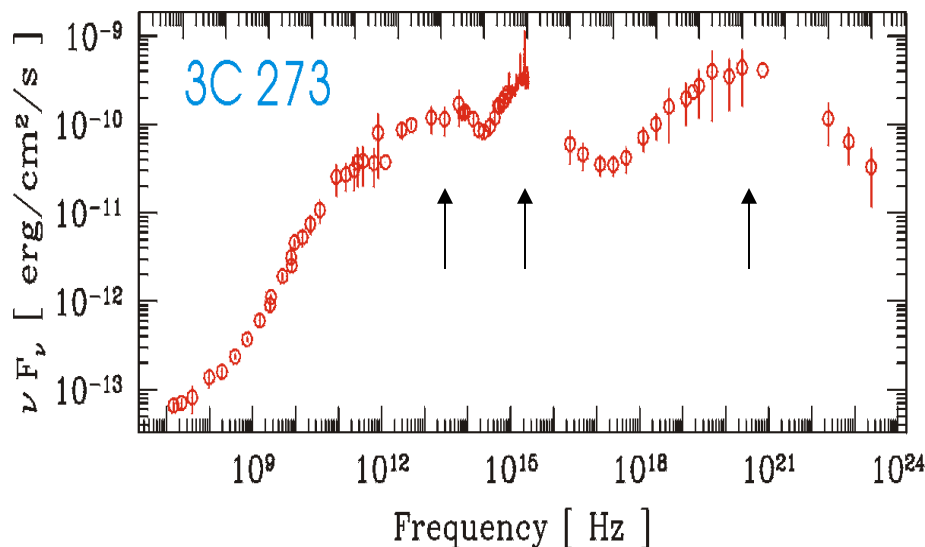
$$\text{cm},$$

$$\Omega_m = 0.3, \Omega_L =$$

$$0.7, h = 0.65$$

Nucleus, Hot Spots, Lobes

(Extranuclear Gamma Rays?)



Gamma-ray
luminosity:

$$\sim 6 \times 10^{46} f_B \text{ ergs s}^{-1}$$

Variability timescale
at gamma-ray
energies:

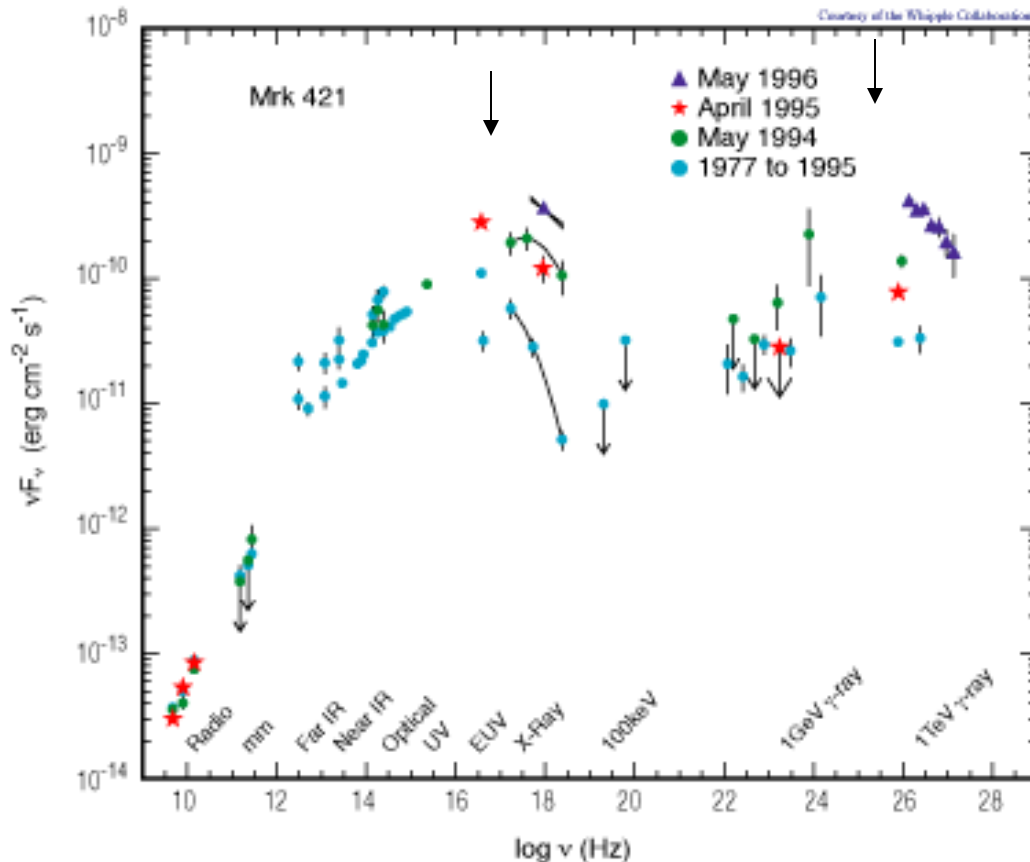
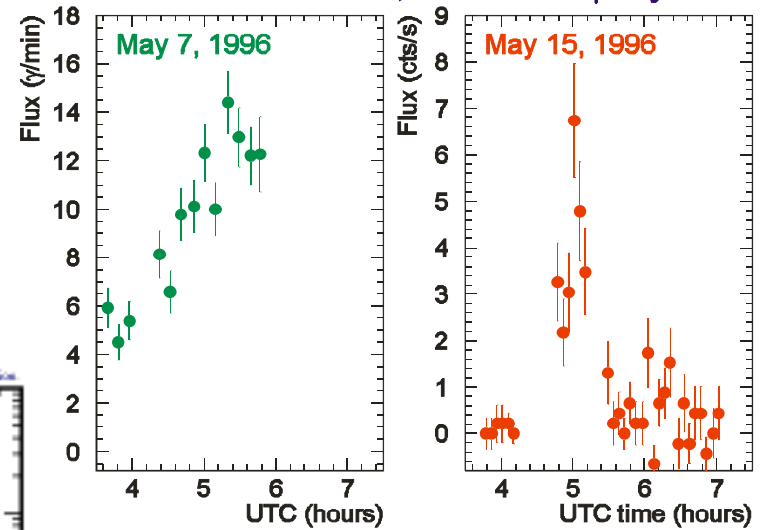
\sim EGRET VP

$$dL/dt \sim 5 \times 10^{40}$$

Nearby BL Lac: Mrk 421



Markarian 421, >300 GeV γ -rays

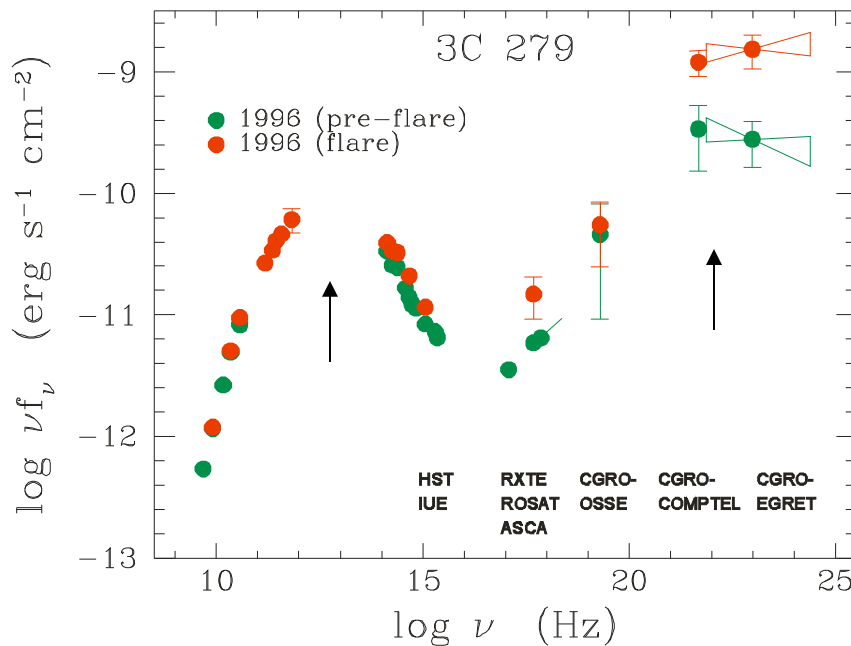
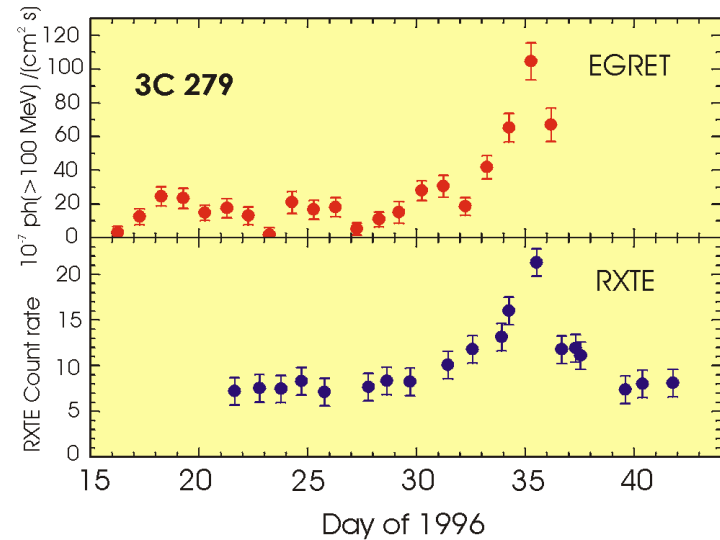
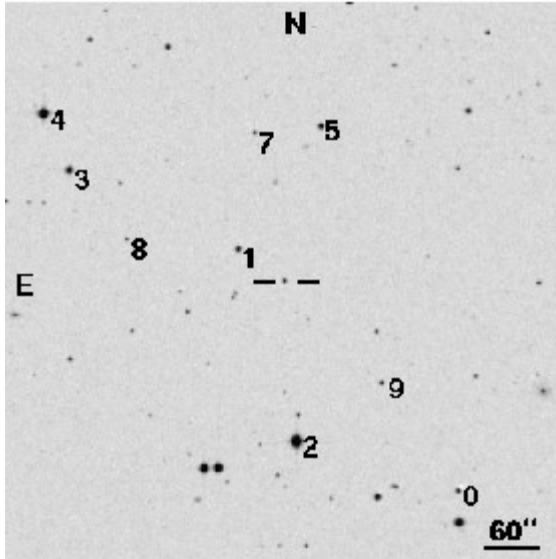


$$z = 0.031, d_L = 4.4 \times 10^{26} \text{ cm}$$

Gamma-ray
luminosity: $\sim 10^{45} f_B$
ergs s⁻¹

Variability timescale
at gamma-ray (TeV)
energies: $\sim 15 \text{ min}$
 $dL/dt \sim 10^{42} \text{ erg / s}^2$

Blazar 3C 279



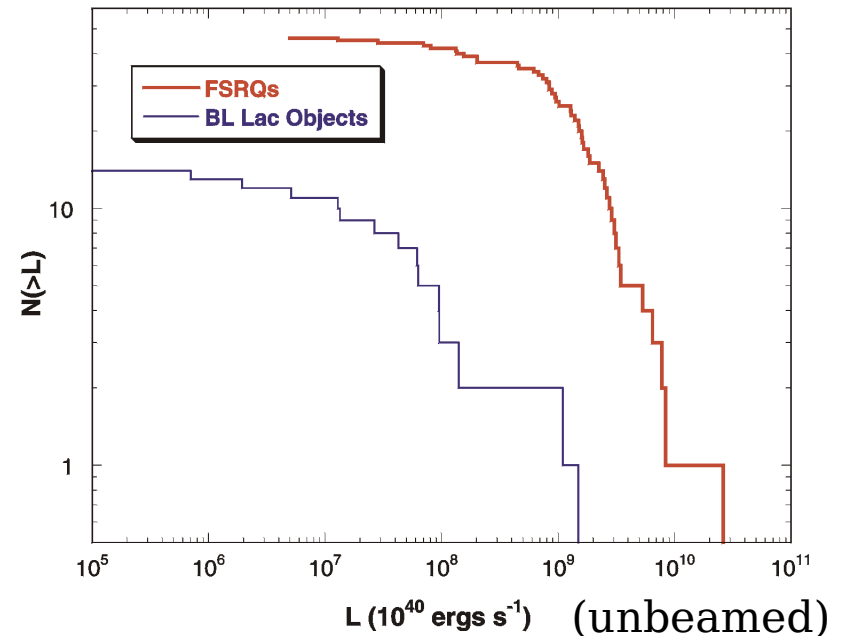
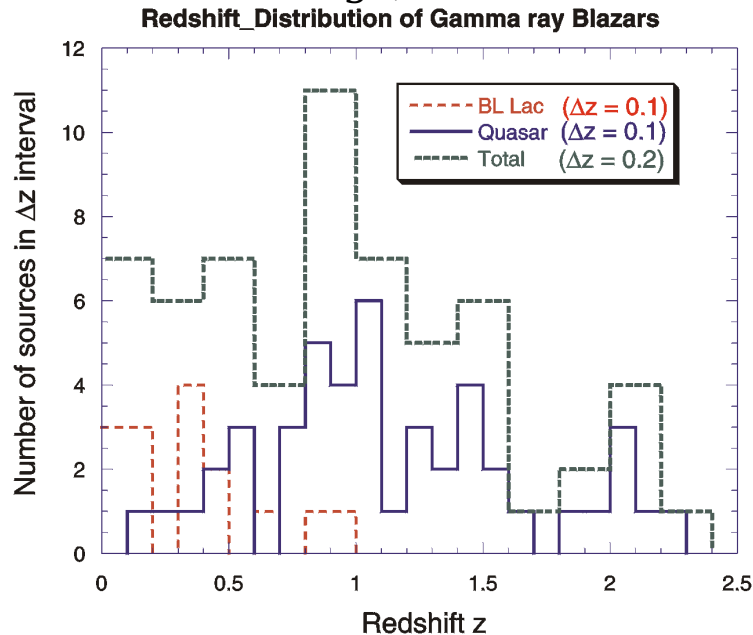
$$z = 0.538, d_L = 8.8 \times 10^{27} \text{ cm}$$

Gamma-ray
luminosity:
 $\sim 5 \times 10^{48} f_B \text{ ergs s}^{-1}$

Variability timescale
at gamma-ray
energies:
"energy acceleration"

Redshift and Luminosity Distribution of Gamma Ray Blazars

Redshift (left) and luminosity (right) distribution of 60 high confidence gamma-ray blazars (14 BL Lac objects and 46 FSRQs) in the Third EGRET catalog (Hartman et al. 1999).

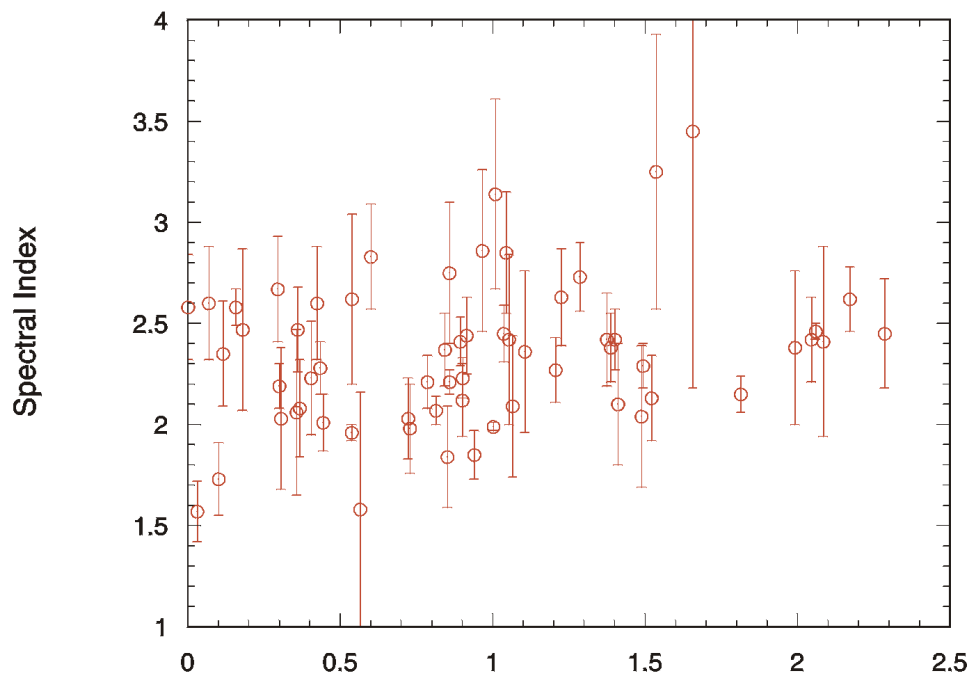


Sources within 10° of the Galactic plane excluded. Catalogs of Padovani & Giommi (1995) and Perlman et al. (1996) used for BL Lac identifications.

- BL Lacs: less numerous and closer, with an average redshift of ~ 0.5
- FSRQs: average redshift peaks at $z \sim 1$, with tail reaching to $z \sim 2.3$.
- Luminosities of FSRQs are 1-2 orders of magnitude greater than those of the BL Lacs
- Thousands of blazars and tens of radio galaxies with GLAST -- depending on population evolution and luminosity functions

Gamma Ray Blazar Spectral Indices

> 100 MeV peak spectral indices from Third EGRET catalog
No evidence for K-correction
Insufficient statistics to examine > 1 GeV spectral indices



GLAST sensitivity can examine > 1^z GeV spectral indices and spectral cutoffs from:

- Intrinsic cutoffs of radiating sources
- $\gamma\gamma$ opacity due to local radiation fields
- $\gamma\gamma$ opacity due to cosmic diffuse radiation fields

Evidence for Relativistic Outflows

1. Synchrotron Self-Compton Limits

(aka Compton catastrophe)

Observe L_{radio} , ν_{radio} , Δt or $\Delta\theta \Rightarrow$ radius R , u_{syn}

Synchrotron self-absorption frequency $\Rightarrow B$ from synchro-Compton theory

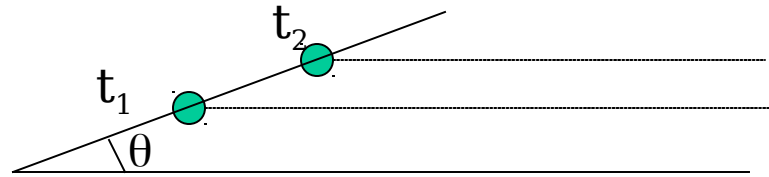
Ratio $u_{\text{syn}} / (B^2/8\pi) \gg 1 \Rightarrow$ large flux of synchrotron self-Compton X-rays (not seen)

Resolution:

Beaming (Woltjer 1966) or

Bulk relativistic motion (Blandford and Rees 1978)

Provides information on bulk outflow at the 0.1-1 pc scale where radio emission is formed (gravitational radius is 10^{-4} pc for 10^9 Solar mass black hole)



2. Apparent Superluminal Motion

$$\Delta t_{\text{obs}} = \Delta t(1 - \beta \cos \theta)$$

$$\Delta x_{\perp} = \beta c \Delta t \sin \theta$$

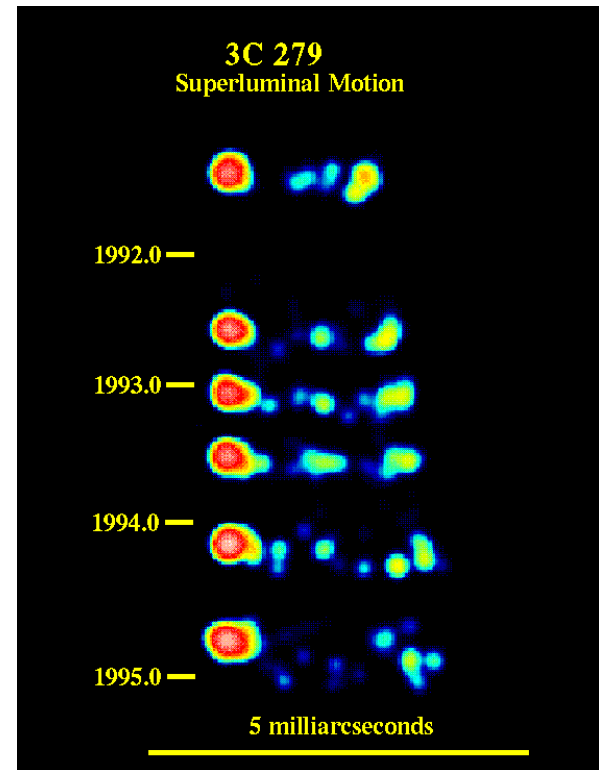
$$\Rightarrow \beta_{\perp} c = \Delta x_{\perp} / \Delta t_{\text{obs}} = \beta c \sin \theta / (1 - \beta \cos \theta)$$

$$\rightarrow \beta \Gamma c$$

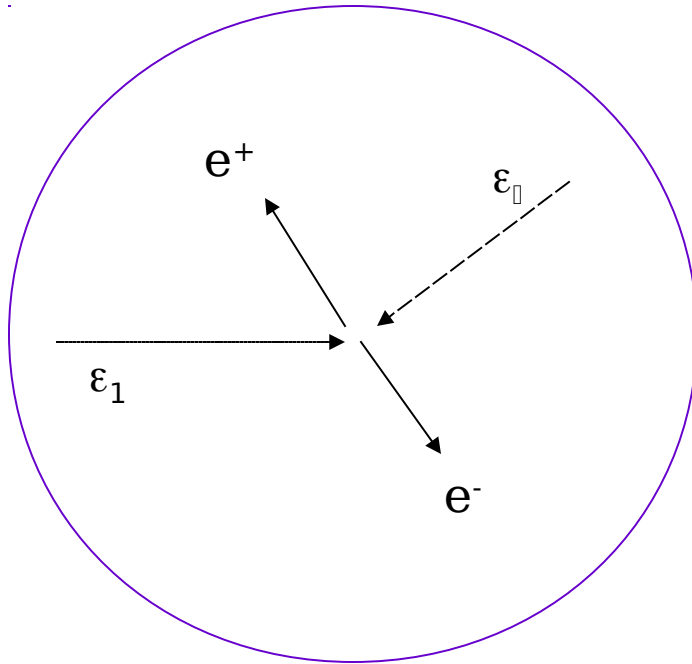
$(\Gamma \gg 1, \theta \approx 1/\Gamma)$

Apparent SL motion now seen from scores of radio sources, with apparent SL speeds typically

between 1 and 10, though with a few reaching ~ 20 (Vermeulen and Cohen 1994)



3. $\gamma\gamma$ Transparency Arguments



Threshold condition

$$s = \epsilon_1 \epsilon_2 = E_1 E_2 / (m_e c^2)^2 > 1$$

Cross section $\sigma_{\gamma\gamma} \approx \sigma_T / s$

For γ -ray transparency ($\epsilon_1 = \epsilon_\gamma$)

$$n_2 \sigma_{\gamma\gamma} R < 1$$

$R \sim c \Delta t_{1,2}$ (correlated observations
or cospatial assumption)

$$n_2 \sim L_2 / [E_2 (4\pi R^2 c)] \Rightarrow$$

$$\Rightarrow \frac{L_2}{\Delta t_{1,2}} < \frac{(4\pi c \epsilon_1 \epsilon_2) E_2}{\sigma_T}, \quad \epsilon_1 \epsilon_2 < \frac{L_2}{[E_2 (4\pi R^2 c)] \sigma_T} < 1$$

$$\epsilon_1 \rightarrow \epsilon_\gamma, \quad \epsilon_2 \rightarrow \epsilon_X, \quad \epsilon_\gamma \epsilon_X \sim 1 \Rightarrow \frac{L_X}{\Delta t_{X,\gamma}} < \frac{4\pi c E_X}{\sigma_T}$$

Probe of site of gamma-ray production (within 10^2 - 10^4 Rs of supermassive black hole)

4. Elliot-Shapiro Relation

Assume stationary emission region

$$L_{\text{Edd}} = 1.26 \times 10^{46} M_8 \text{ ergs s}^{-1}$$

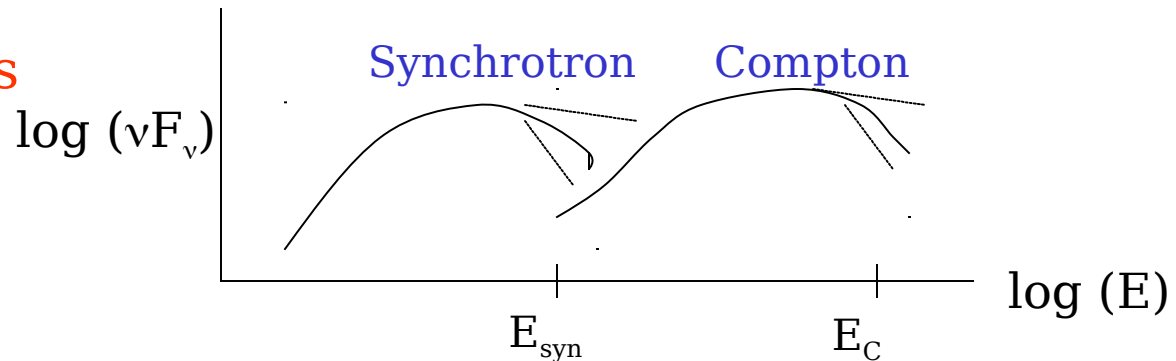
$$\Delta t > R_s/c \approx 3 \times 10^{13} M_8 / c \approx 10^3 M_8 \text{ s}$$

$$\square L / \Delta t < 10^{43} k_C \text{ ergs s}^{-2}; k_C \text{ corrects for Klein-Nishina effects}$$

(Dermer and Gehrels 1995)

5. Other tests

(Catanese et al.
1997)



Correlated variability between optical/X-ray and GeV/TeV

1. Observation of synchrotron and Compton cutoffs $\Rightarrow B \approx 2E_{\text{syn}}(\text{eV}) \delta / [E_C(\text{GeV})]^2$

2. Variability of synchrotron component (assumed due only to synchrotron radiation) $\Rightarrow [E_{\text{syn}}(\text{eV}) \delta \Delta t(\text{day})]^{1/3} < B(\text{Gauss}) < 2E_{\text{syn}}(\text{eV}) \delta / [E_C(\text{GeV})]^2$

Violation \Rightarrow beaming

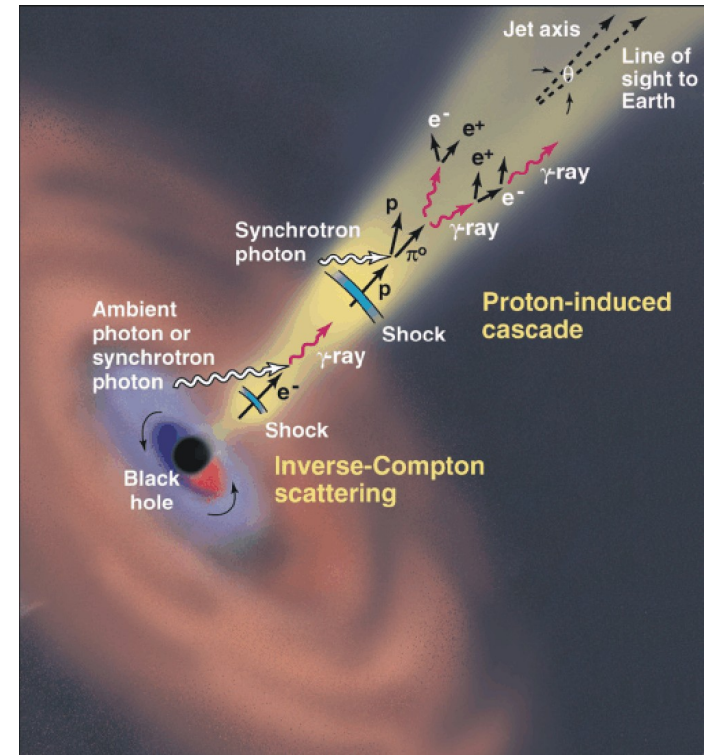
Particle Radiation and Acceleration Processes in Blazar Jets

Standard Blazar Model:

- collimated ejection of plasma with small baryon loading (i.e., bulk Lorentz factor $\Gamma \gg 1$)
- reconversion of directed outflow kinetic energy through internal or external shocks
- particle acceleration and radiation

Radiation:

- peaks in SED: nonthermal synchrotron and Compton (SSC, external Compton, reflected Compton) components, blue bump, dust component



(courtesy J. H. Buckley)

Beaming pattern:

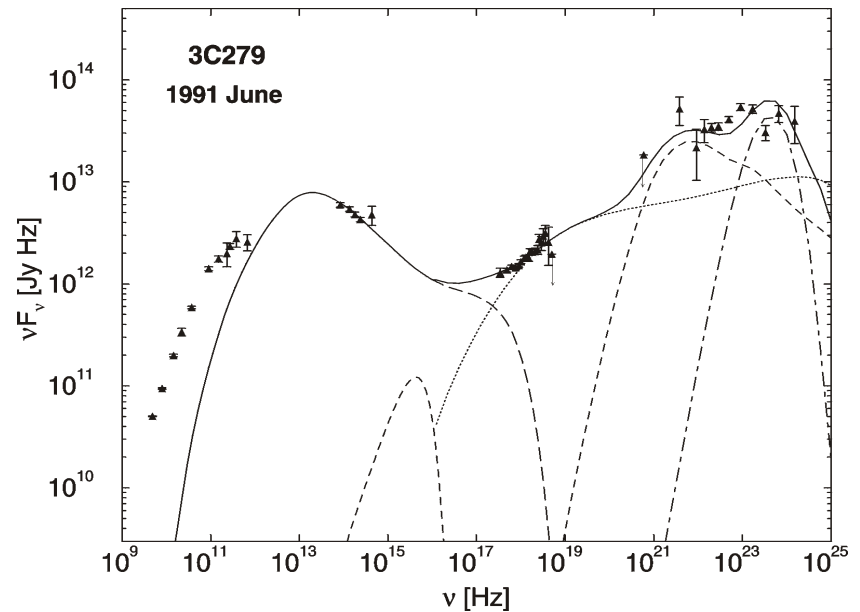
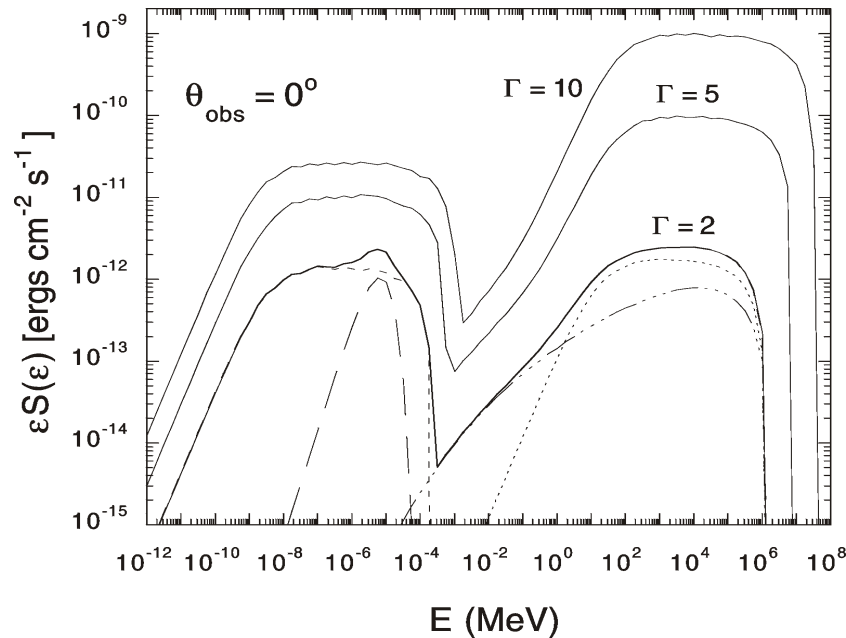
Radiating Particles

- synchrotron and SSC. Flux density $F \propto \delta^{1+\alpha}$
- primary electrons

- secondary leptons from hadrons which form cascade through external Compton. $F \propto \delta^{1+\alpha}$
- photomeson, photopair, and proton synchrotron emission

$\delta = 1/[\Gamma(1-\beta\cos\theta)]$ is Doppler factor

Spectral Modeling



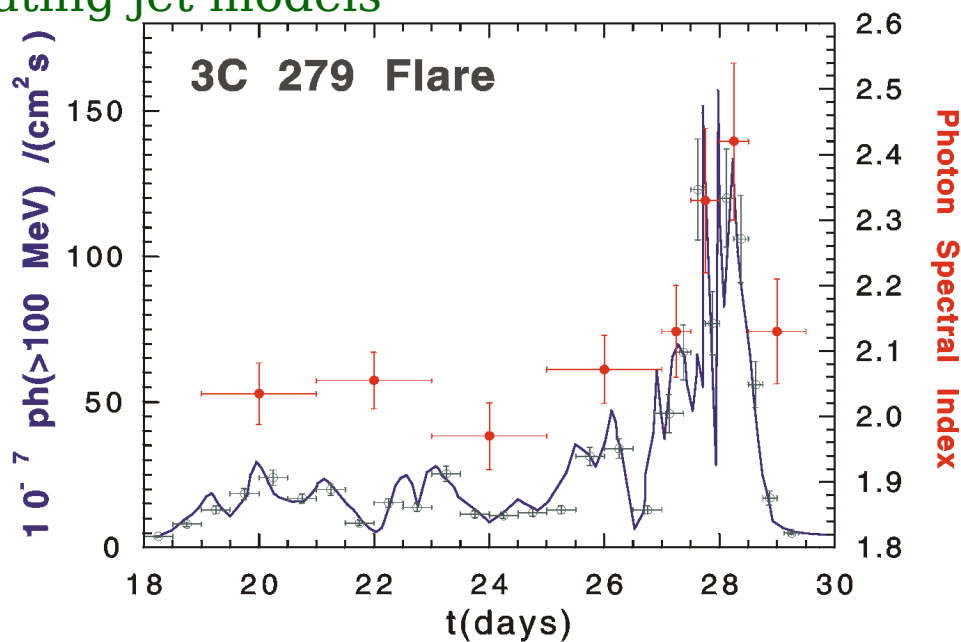
Leptonic radiation processes: parameters studies \rightarrow ranges of Doppler factors and magnetic field strengths in pure SSC models

Detailed spectral variations result from multiple radiation components (e.g., PKS 0529+134; Böttcher and Collmar 1998)

Correlated variability \rightarrow information on acceleration and

Variability Studies of Blazars with GLAST

Using beaming tests, GLAST observations can chart the variation of Doppler factor with time; test accelerating and decelerating jet models



- Spectral index/flux behavior
- E_{pk} /flux behavior
- Spectral index/ E_{pk} behavior

Important to probe
correlated γ /X behavior

Statistics of Blazars

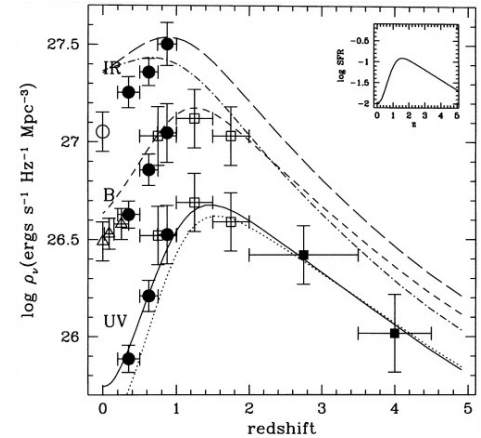
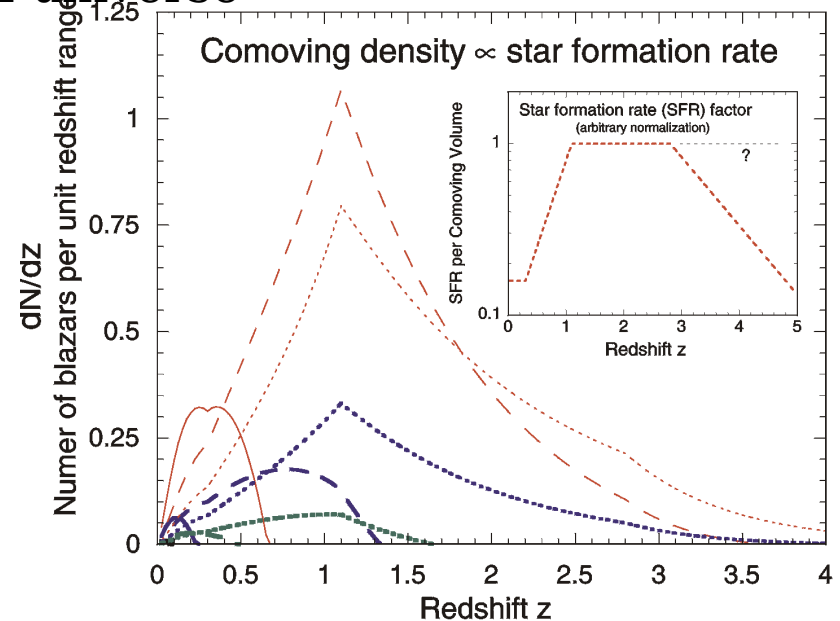
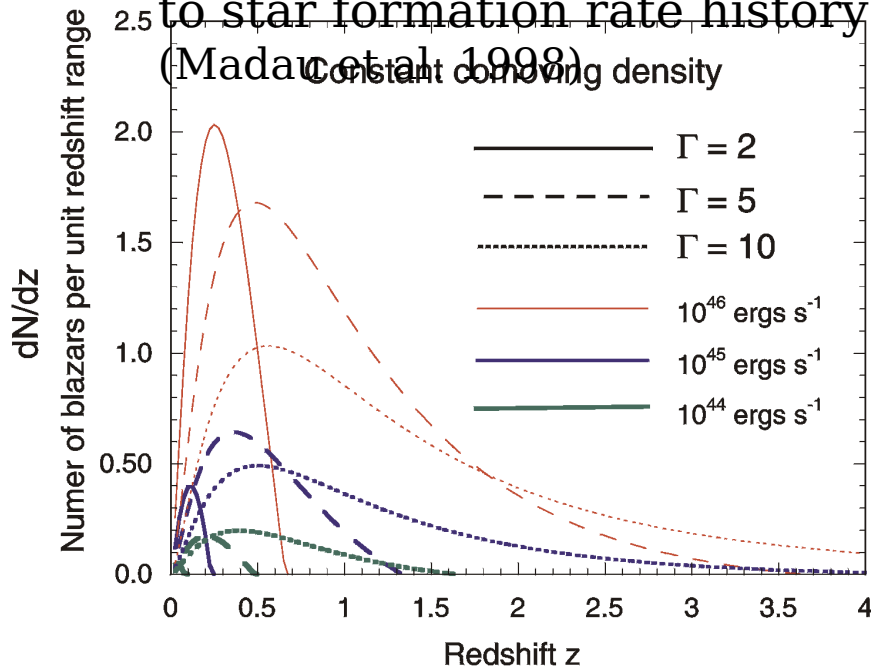
(Dermer and Davis 1999)

Based on model of Dermer and Gehrels (1995):

- randomly oriented, collimated relativistic plasma blobs
- beaming pattern given by $F \propto \delta^{\Gamma+\alpha}$
- Comoving density of blazars proportional

to star formation rate history of universe

(Madau et al 1998)

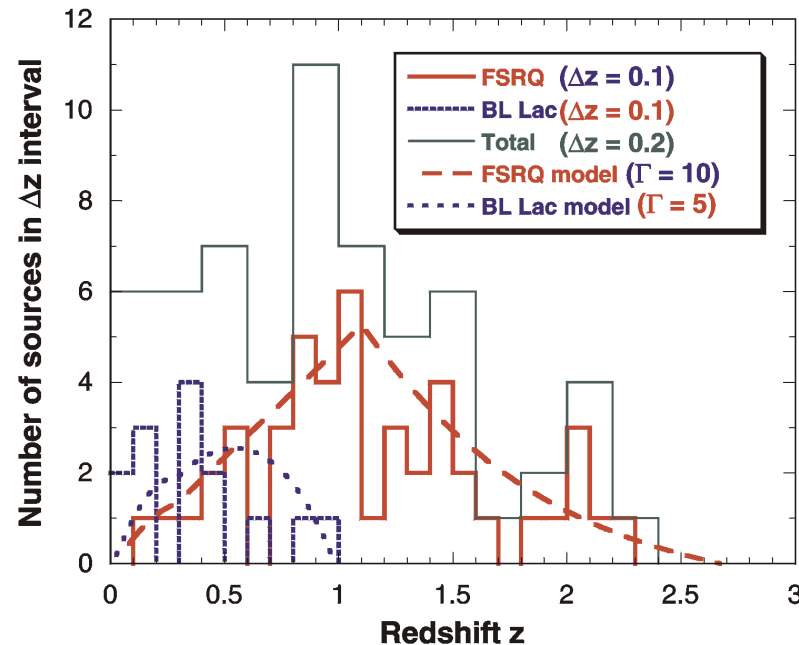


Model fitting depends only on comoving luminosity in blob and bulk Lorentz factor of blob, and assumption about source density with redshift

(approach differs from Chiang & Mukherjee (1998) by considering density rather than

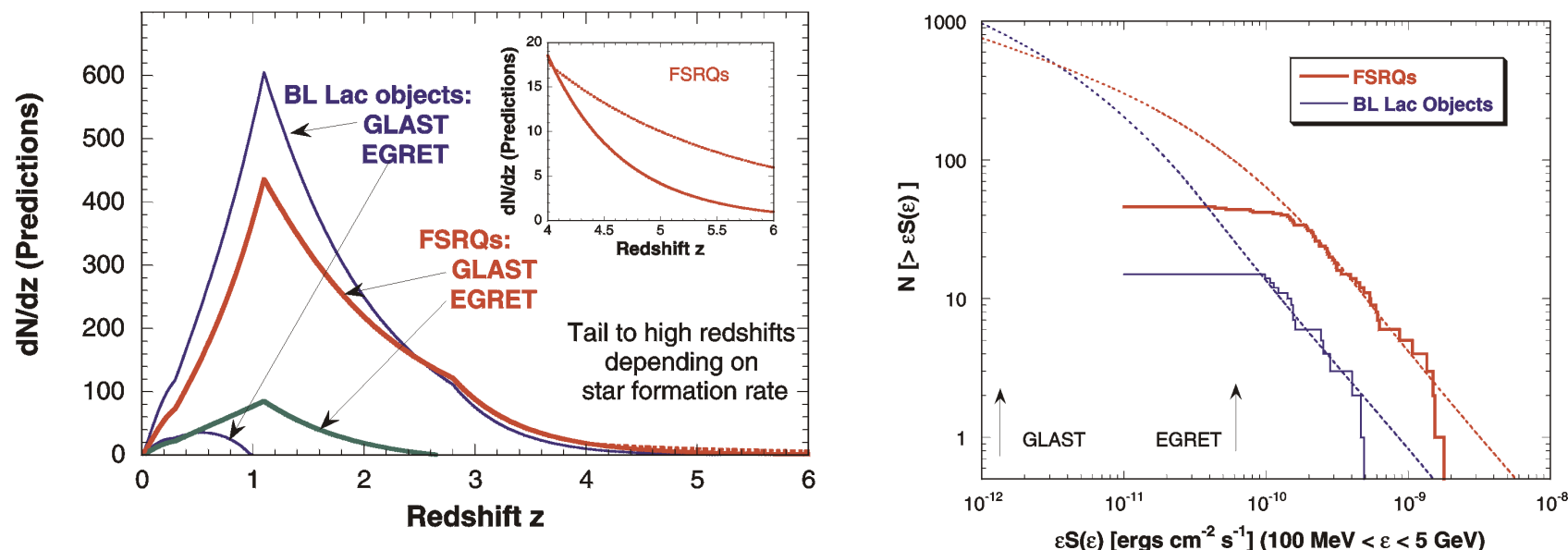
Fit to Redshift Distribution of Blazars

Redshift distributions for constant comoving density model does not give good fit to the data (especially for the FSRQs): it peaks at too small a redshift



Model with blazar density proportional to SFR give a good fit to the redshift and flux distributions

Predicted Redshift and Flux Distribution Observed with GLAST



Extrapolating to the flux threshold for GLAST \Rightarrow GLAST should detect ~ 2000 blazars and a larger fraction (50% rather than the 25% observed with EGRET) should be BL Lac objects.

Predict a flowering of BL Lac objects with GLAST

Most will be “high-frequency peaked” BL Lac objects, many of which will not have been previously identified, and will provide a rich new class of targets for TeV observatories.

Blazars contribute large ($> 20\%$) fraction of extragalactic gamma

Black Hole/Accretion Disk/Jet Physics

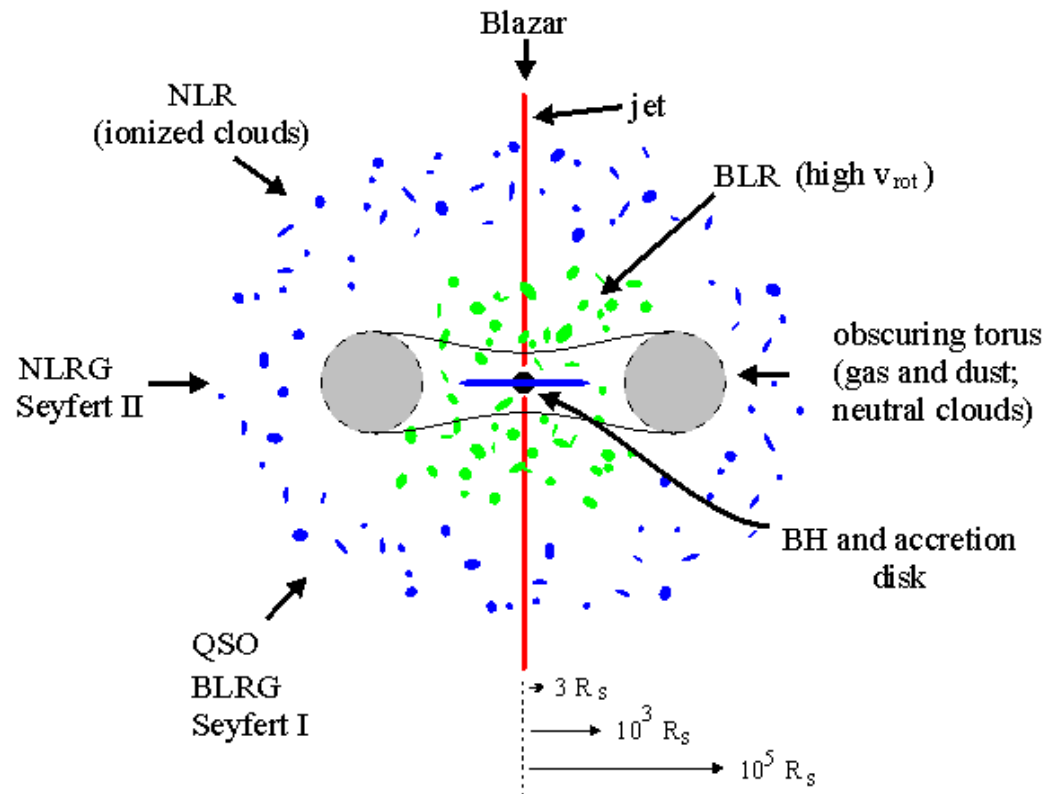
Jet origin: Poynting flux
(Blandford-Znajek process),
pair outflow, exhaust gas --
composition of jet

Jet collimation: magnetic vs.
hydrodynamic

Inner jet models:
Accelerating vs. decelerating
jet models

Disk-jet symbiosis (galactic
microquasar studies):
Relationship of jet power to
disk power (Falcke et al.)

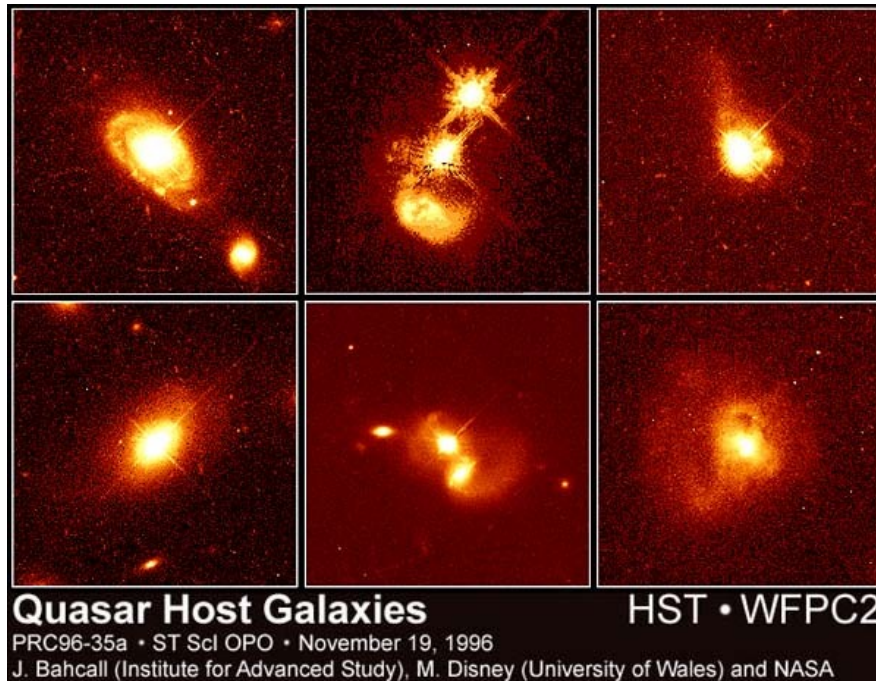
Reverberation mapping:
GLAST may discover imprint
of disk radiation in attenuated
GeV emission (Böttcher and



Relationship to Galaxies and AGN

Unification by Evolution: Spiral \rightarrow IR luminous \rightarrow Quasar/Blazar \rightarrow E

Origin of intense IR emission in IR luminous galaxies (buried starbursts)



Buried blazars as intense gamma-ray sources with weak associated X-ray sources

Morphological studies of host galaxies of different classes of blazars (e.g., FSRQ, RBL, XBL) to test galaxy evolutionary scenarios

Physical origin of trend identified by Sambruna et al. (1996) and Fosbury et al. (1998) that luminosity decreases with increasing E_{pk}

Ultra-High Energy Cosmic Rays and Neutrinos

Origin of super GZK cosmic rays: acceleration in the jets of radio galaxies (Rachen and Biermann 1993)

UHECRs arrival directions correlated with directions to sources

Generation of pair cascades and neutron decays

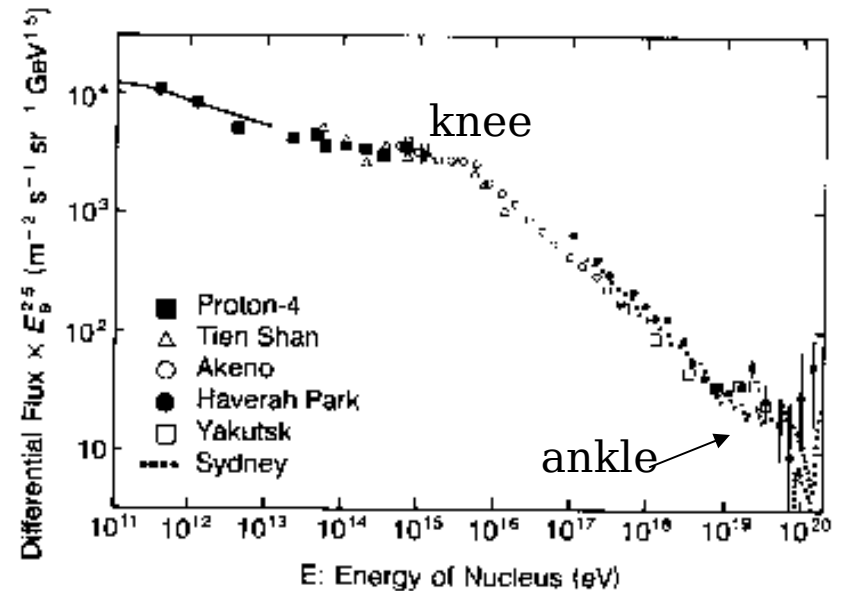
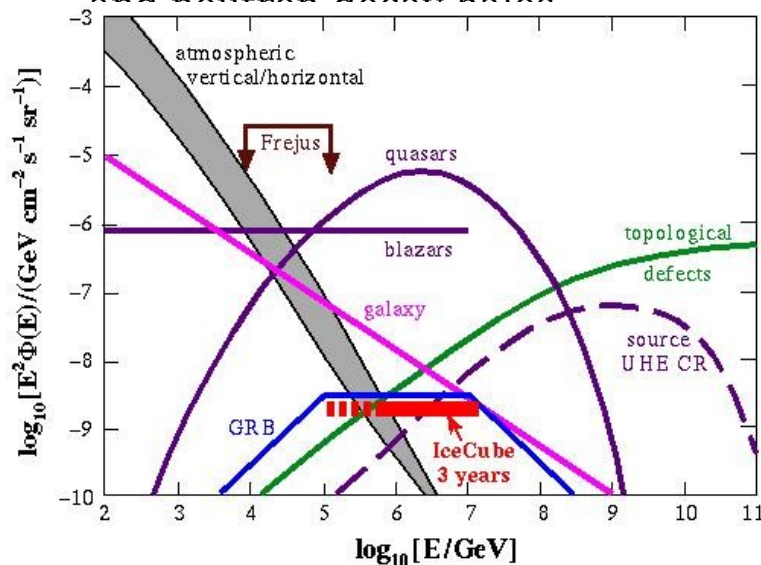


Figure 2. Cosmic ray energy spectrum multiplied by $E^{2.5}$ to better show the spectral variations. (Adapted from Hillas, 1984.)

Neutrinos from Blazars:

Amanda II, ICE Cube, and deep underwater high energy neutrino detectors will provide detections of or limits on proton acceleration in blazars

Blazars as Probes of the Diffuse Intergalactic Infrared Radiation Field

$\gamma + \gamma_{\text{IR}} \rightarrow e^+ e^-$ cutoff probes DIIRF

$E(\text{TeV}) \lambda (\mu\text{m}) \approx 2.5$

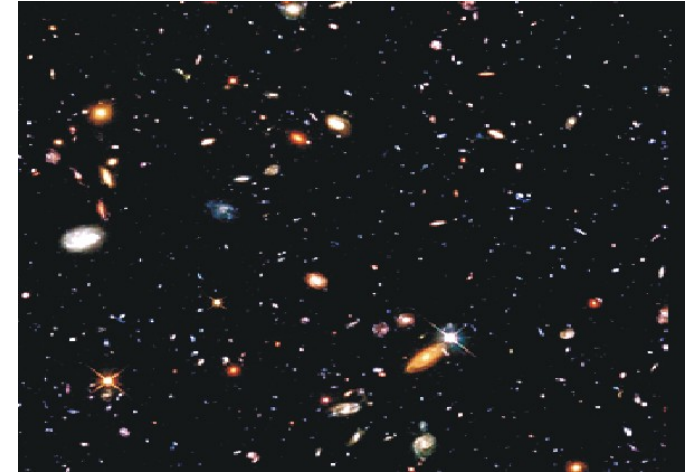
Consistent with lack of detection of TeV γ rays from $z > 0.3$ blazars (so far detected at > 300 GeV from Mrk 421 at $z = 0.031$, Mrk 501 at $z = 0.034$, 1ES 2344+514 at $z = 0.044$, PKS 2155-304 at $z = 0.117$, and 1H1426+428 at $z = 0.129$)

DIIRF difficult to observe directly due to:

Zodiacal light, IR Cirrus, and CR electron synchrotron

Cosmological significance of DIIRF: Integrated reprocessed stellar and AGN radiation since onset of galaxy formation

Pair absorption cutoffs at low redshifts provide integral IR emission due to galactic emission; pair absorption cutoffs at high redshifts provide differential measure of DIIRF



HDFS

GLAST Strategies

1. Time Series Analysis of Blazar Data

Periodic/QPO

2. Time Correlation Studies

Cross Frequency/Long Baseline

3. Subtraction of Variable Background

Upper limits to
nonvariable components

4. Occultation analysis

Angular Resolution
Enhancement